Energy partitioning in the reaction $^{16}O(^1D)+H_2{}^{18}O \rightarrow {}^{16}OH+{}^{18}OH$. IV. Microscopic probabilities for $^{16}OH+{}^{18}OH$ coincident pairs

F. J. Comes and K.-H. Gericke

Institut für Physikalische und Theoretische Chemie der Universität, 6000 Frankfurt am Main, West Germany

J. Manz

Lehrstuhl für Theoretische Chemie, Technische Universität München, 8046 Garching, West Germany
(Received 5 May 1981; accepted 1 June 1981)

The reaction $^{16}O(^1D) + H_2{}^{18}O \rightarrow {}^{16}OH(^{16}f) + {}^{18}OH(^{18}f)$ yields product molecules with internal [i.e., rotational (j), electronic (Ω), and vibrational (v)] levels ^{16}f and ^{18}f. The corresponding populations $^{16}P(^{16}f)$ and $^{18}P(^{18}f)$ are determined experimentally by photochemical preparation of reactants and detection of products after a 10 ns delay. Using this information, we predict the joint probabilities $P(^{18}f, ^{16}f)$ of observing the product pair simultaneously. For this purpose, we exploit that (a) summations of the less resolved joint vibrational probabilities $P(^{18}v, ^{16}v)$ over ^{18}v or ^{16}v yield exactly the observed vibrational populations $^{16}P(^{16}v)$ or $^{18}P(^{18}v)$, respectively; (b) a fraction of the nonvibrational energy of the $(^{18}v, ^{16}v)$ pair is released as rotational energy; and (c) the product molecules rotate with approximately opposite angular momenta $^{16}j \approx -{}^{18}j$ due to the kinematics of light atom transfer. Imposing the constraints (a)–(c), information theory is used to determine $P(^{18}f, ^{16}f)$ such that the summations over ^{18}f or ^{16}f yield optimal agreement with the experimental $^{16}P(^{16}f)$ or $^{18}P(^{18}f)$, respectively. The results show that (a) simultaneous vibrational excitation of the product pair is negligible, i.e., vibrational energy release is very specific; (c) specific rotational energy release increases with vibrational excitation; and (c) the internal distribution of vibrationally excited OH radicals also contributes to the internal distributions of their $v = 0$ partners.

I. INTRODUCTION

In this paper we present for the first time microscopic reaction probabilities for two coincident product molecules emerging from a chemical reaction. The results are obtained for the isotopically labeled systems

$$^{16}O(^1D) + H_2{}^{18}O \rightarrow {}^{16}OH(^{16}f) + {}^{18}OH(^{18}f) \qquad (1.1)$$

which plays a significant role in atmospheric chemistry.[1] Reaction (1.1) is exothermic, Here, f denotes the rotational (j),[2] electronic (Ω), and vibrational (v) states. The two distributions $^{16}P(^{16}f)$ and $^{18}P(^{18}f)$ have been measured experimentally,[3,4] as has the overall reaction rate coefficient.[5] This was done with the aid of a tunable narrow bandwidth UV laser which allowed determining not only the population of OH product molecules in the accessible vibrational and rotational states but also their translational energy distribution. In addition, the high resolving power made possible a separate discussion of the effect of electron and nuclear spin on the reaction probability. Some information on the product distributions has also been presented in Refs.[6–9] We determine $P(^{18}f, ^{16}f)$, the *joint* probability of simultaneously observing $^{16}OH(^{16}f)$ *and* $^{18}OH(^{18}f)$. Clearly, $P(^{18}f, ^{16}f)$ provides more detailed information on process (1.1) than $^{16}P(^{16}f)$ and $^{18}P(^{18}f)$, because the internal distribution of one radical is only the sum of $P(^{18}f, ^{16}f)$ over all internal levels of the other radical:

$$^{16}P(^{16}f) = \sum_{^{18}f} P(^{18}f, ^{16}f) \qquad (1.2)$$

and

$$^{18}P(^{18}f) = \sum_{^{16}f} P(^{18}f, ^{16}f) \; . \qquad (1.3)$$

Correspondingly, it is more difficult to determine $P(^{18}f, ^{16}f)$ than just $^{16}P(^{16}f)$ and $^{18}P(^{18}f)$. In the present work, we use a simple model, together with the very detailed experimental information on $^{16}P(^{16}f)$ and $^{18}P(^{18}f)$, to predict the joint probabilities $P(^{18}f, ^{16}f)$ with the help of information theory.[10]

A direct experimental measurement of $P(^{18}f, ^{16}f)$ would require the simultaneous determination of $(^{18}f, ^{16}f)$ *coincident* events. In this respect, reactions with two molecular products, such as Eq. (1.1), are fundamentally more complicated than reactions of the three center type

$$A + BC \rightarrow AB(f) + C \; , \qquad (1.4)$$

which yield an atom and a diatomic molecule as products. In the latter it suffices, in principle, to measure the molecular distribution, since the coincident atomic one is determined by conservation laws (for given initial conditions). Not so for the present system, where even complete knowledge of both product molecular distributions is not sufficient to determine uniquely the joint probabilities of coincident events.

An alternative determination of $P(^{18}f, ^{16}f)$ is possible, in principle, by measuring the reactivity of the reverse reaction. This would require exciting both hydroxyl radicals into fully state resolved *reactant* levels $(^{18}f, ^{16}f)$, e.g., with the help of lasers. The data could then be converted into $P(^{18}f, ^{16}f)$ using detailed balance.[11,12] However, such experiments using double excited pairs of reactants are only in their beginnings. So far they have yielded, at best, a very small number of matrix elements $P(^{18}f, ^{16}f)$ for a few systems.[13] In contrast, the present work aims at determining the full joint probability matrix. In principle, $P(^{18}f, ^{16}f)$ could also be obtained by purely theoretical methods, but to the best of our knowledge the full power of, say, class-

 0021-9606/81/182853-11$01.00

ical trajectory or even just statistical techniques has not yet been exploited for this purpose (see Refs. 14–16 for some less resolved applications of these techniques to reactive A+BCD – AB+CD systems, and Ref. 17 for the first fully resolved joint vibrational probability matrix evaluated for the collinear $O+CS_2 \rightarrow SO+CS$ model reaction with the help of classical trajectories). This paper is structured as follows. In Sec. II, we briefly summarize the relevant experimental results. The theory is presented in Sec. III, the results and the discussion in Sec. IV, and the conclusions in Sec. V.

II. EXPERIMENTAL

Our experiment employs a fast system of photochemical production and detection, which utilizes nanosecond spectroscopy to investigate the unperturbed distributions of the two product molecules ^{16}OH and ^{18}OH.[4] To this end, ozone in an O_3–H_2O mixture is photolyzed by a nanosecond UV beam produced as the fourth harmonic of the output of a Nd:YAG laser

$$^{16}O_3 + h\nu\,(266\text{ nm}) \rightarrow {}^{16}O(^1D) + {}^{16}O_2(^1\Delta_g)\ . \qquad (2.1)$$

The resulting $^{16}O(^1D)$ atoms react with isotopically labeled water ($H_2{}^{18}O$) at a gas-kinetically determined rate[5] to form ^{16}OH and ^{18}OH according to Eq. (1.1). These products are analyzed after a 10 ns delay by a pulsed and frequency doubled dye laser. Detection of the "nascent" OH radicals is accomplished by measuring the absorption resulting from their resonant transitions $A\,^2\Sigma^+(f) - X\,^2\Pi(f)$. The absorption technique is the only practicable method of quantitatively determining OH in vibrational levels higher than $v''=1$, for the lifetimes of $A\,^2\Sigma^+(v'>1)$ are significantly reduced by predissociation.[18–20] This is also true for very high j values of lower vibrational states ($v'=0,1$). This instability sharply reduces the fluorescence efficiency, but does not measurably affect the absorption line width, which in the present experiment is determined by the Doppler effect. Investigating the initial distribution of OH product molecules by means of absorption spectroscopy has further advantages over the previously discussed fluorescence method. Quenching and energy transfer processes in the fluorescing state can appreciably influence the fluorescence yield—an effect which plays no role whatsoever in absorption. For sample gas pressures in the commonly used range 0.1–1 Torr, the effect of these collision processes is already so large that the radiative lifetime of the OH radicals in the $A\,^2\Sigma^+$ state can be diminished as much as 50%. This has a great effect on the data whenever the effectiveness of collisions depends on the quantum state of the colliding molecule or whenever the radiative lifetime of the molecule depends on its quantum state.[21,22] Both conditions apply to OH in its $^2\Sigma^+$ state, and it has already been pointed out that the latter practically excludes the possibility of observing OH molecules in vibrational states with $v''>1$ by fluorescence methods. The relatively high temperature observed by Butler *et al.*[8] for the rotational distributions of OH from reaction (1.1) may be attributable to this situation. According to Lengel and Crossley[21] it is to be expected that the effect of these collision processes will distinctly decrease with increasing rotational excitation, which also means that a higher apparent rotational population, and thus a higher rotational temperature, will be observed. It may also be noted that the authors, in an earlier publication[7] cited a lower rotational temperature. The resulting conclusion in Ref. 8, that the rotational distribution is nearly statistical, is a consequence of the use of a too low available energy in calculating the prior probabilities.

The simple structure of the OH molecule permits a complete analysis of the product state distribution, including such fine details as the distribution over the several Λ components, and over different electron spin and nuclear spin states. In the present paper, however, not all of these details are required. The reported results are therefore obtained by summation over the lambda and hyperfine levels, so that the reported resolution (j,Ω,v)[23] is

$$^{16,18}P(j,\Omega,v) = \sum_{\Lambda}\sum_{I} {}^{16,18}P(j,\Lambda,I,\Omega,v)\ . \qquad (2.2)$$

The observed densities of states of the product molecules were obtained with a pulsed laser system. Hence they are proportional to the reaction probabilities P which are used in this paper. The locations of the absorption lines, as well as the transition probabilities for Eq. (2.2), were taken from the literature.[24–28] The values of the energy levels for ^{16}OH were taken from Ref. 24, and those for ^{18}OH from Ref. 28. The measured peak heights of a scan[4] over the individual absorption lines show an uncertainty of 15%. In unfavorable cases, i.e., for very small absorptions and isolated lines between vibrational bands, the uncertainty can reach 30%. Since, however, the values used in the calculations are derived from several experimental data, the standard error is distinctly smaller.

The observed reaction probabilities are presented in their original form, without smoothing or any numerical reduction of the relaxation phenomena. This is done mainly because one of the conclusions of this paper is that such manipulations require great care; consequently the data of this work differ slightly from those of Ref. 4.

The product state distributions are not sensitive to the total product energy E. This conclusion is drawn from a series of experiments with argon added as a buffer gas. As a consequence, the translationally hot $O(^1D)$ atoms nascent from ozone photolysis are cooled down to thermal energies without influencing significantly the title reaction.

III. THEORY

A. Energetics

The title reaction is subject to several kinematic constraints. In this subsection we exploit energy conservation. Angular momentum conservation will be considered later in Sec. III D. The total energy available to the products is

$$E = E_{\rm int} + E_{\rm trans} + \Delta E\ . \qquad (3.1)$$

Here $E_{\rm int}$ is the internal reactant energy. For $H_2{}^{18}O$ at $T=300$ K,

$$E_{int} \simeq 3RT = 7.5 \text{ kJ mol}^{-1} ; \quad (3.2)$$

E_{trans} is the translational energy of the reactants (see Appendix A)

$$E_{trans} \simeq 22.6 \text{ kJ mol}^{-1} ; \quad (3.3)$$

E is the ground-state-to-ground-state exoergicity[29]

$$\Delta E = 117.4 \text{ kJ mol}^{-1} . \quad (3.4)$$

Thus

$$E \simeq 147.5 \text{ kJ mol}^{-1} . \quad (3.5)$$

Actually E_{int} and E_{trans} have thermal and nonthermal distributions, respectively (see Appendix A and Ref. 31), implying a corresponding distribution of E. Nevertheless, the use of the approximation of a fixed total energy (3.5) is justified for the following reasons. Firstly, our preliminary experimental results indicate that the reaction dynamics of the title system is not very sensitive to variations of the energy (cf. Sec. II). Secondly, the subsequent theoretical results do not depend dramatically on values of E between 135 kJ mol^{-1} and 155 kJ mol^{-1}, the range of dominant contributions to the distribution of E. This energetic insensitivity is mainly a consequence of the large exoergicity of the title reaction.[32]

The available energy (3.5) is transferred into the translational and internal energies of the products

$$E = E_{trans} + {}^{16}E({}^{16}f) + {}^{18}E({}^{18}f) . \quad (3.6)$$

This expression of energy conservation has a consequence which is almost trivial, yet very important in practice: The number of accessible product states $({}^{18}f, {}^{16}f)$ is finite (albeit quite large, $\simeq 8000$). Hence the probability matrix $P({}^{18}f, {}^{16}f)$ is finite. It is helpful to explain this important consequence by a consideration of the less resolved joint probabilities $P({}^{18}v, {}^{16}v)$ of observing radicals $^{18}OH(^{18}v)$ and $^{16}OH(^{16}v)$ with vibrational levels ^{18}v and ^{16}v, respectively,

$$P({}^{18}v, {}^{16}v) = \sum_{{}^{18}\Omega=1/2} \sum_{{}^{18}j} \sum_{{}^{16}\Omega=1/2} \sum_{{}^{16}j} P({}^{18}f, {}^{16}f) , \quad (3.7)$$

where the sums are over all nonvibrational internal quantum numbers. Let $^{16}E(^{16}v)$ and $^{18}E(^{18}v)$ denote the corresponding vibrational energies. ($E(\vec{v})$ is the minimum energy value of the $E(j, \Omega, v = \vec{v}) -$manifold.) Then Eq. (3.6) implies

$$E > {}^{16}E({}^{16}v) + {}^{18}E({}^{18}v) \quad (3.8)$$

or

$$3 > {}^{16}v + {}^{18}v . \quad (3.9)$$

Equation (3.9) follows from Eq. (3.8) due to the value E, in Eq. (3.5) and the large vibrational level spacing of OH radicals, $\Delta E(v) \simeq 42$ kJ mol^{-1}. These relations (3.8) and (3.9) are illustrated, together with some additional information that will be used later, in Fig. 1. One readily sees that there are, in principle, no more than ten nonvanishing $P({}^{18}v, {}^{16}v)$'s, namely, those implied by the inequality (3.9).

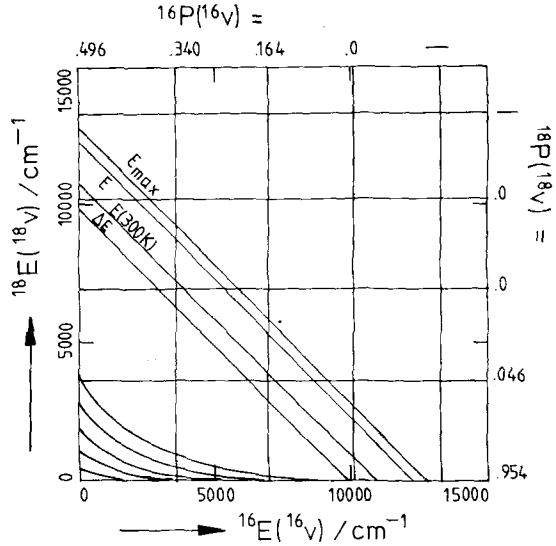

FIG. 1. Triangle plot of joint vibrational reaction probabilities $P({}^{18}v, {}^{16}v)$ for the reaction $^{16}O(^1D) + H_2{}^{18}O \rightarrow {}^{16}OH(^{16}v) + {}^{18}OH(^{18}v)$. Interpolated curvilinear contours for $P({}^{18}v, {}^{16}v) = 0.45$, 0.35, 0.25, 0.15, and 0.05 are shown in this order from bottom to top. The abscissa and ordinate show the vibrational energies $^{16}E(^{16}v)$ and $^{18}E(^{18}v)$ of the product radicals, respectively. The intersections of the corresponding vertical and horizontal lines indicate the total vibrational energy in the $({}^{18}v, {}^{16}v)$ product pair, which in turn is bounded by the average total energy indicated by the straight line marked E. As a consequence, only ten joint vibrational pairs below line E are energetically accessible. Three additional straight lines marked ΔE, E(300 K), and E_{max} show the exoergicity, the average energy for thermal reactants, and the maximum energy of the present nonthermal distribution of reactants, respectively. The experimental values for the internal vibrational distributions $^{18}P_{expt}(^{18}v)$ and $^{16}P_{expt}(^{16}v)$ are given at the right-hand side and at the top, respectively. They are obtained as sums of the joint $P({}^{18}v, {}^{16}v)$ along the horizontal and vertical lines, respectively.

B. Sum rules

Next to the constraint of energy conservation, the experimentally determined internal product molecule distributions impose further constraints on the joint probabilities of coincident events. To illustrate this point let us again first consider just the vibrational analog of Eq. (1.2):

$$ {}^{16}P_{expt}({}^{16}v) = \sum_{{}^{18}v=0}^{3-{}^{16}v} P({}^{18}v, {}^{16}v) , \quad 0 \le {}^{16}v \le 3 , \quad (3.10)$$

$$ {}^{18}P_{expt}({}^{18}v) = \sum_{{}^{16}v=0}^{3-{}^{18}v} P({}^{18}v, {}^{16}v) , \quad 0 \le {}^{18}v \le 3 . \quad (3.11)$$

(The subscript "expt" denotes "experimental".) Here $^{16}P_{expt}(^{16}v)$ is the probability of observing $^{16}OH(^{16}v)$ in vibrational level ^{16}v, irrespective of the other quantum numbers

$$ {}^{16}P_{expt}({}^{16}v) = \sum_{{}^{16}\Omega=1/2}^{3/2} \sum_{{}^{16}j} {}^{16}P_{expt}({}^{16}f) , \quad (3.12)$$

and similarly for $^{18}OH(^{18}v)$,

$$ {}^{18}P_{expt}({}^{18}v) = \sum_{{}^{18}\Omega=1/2}^{3/2} \sum_{{}^{18}j} {}^{18}P_{expt}({}^{18}f) . \quad (3.13)$$

The experimental values of $^{16}P_{expt}(^{16}v)$ and $^{18}P_{expt}(^{18}v)$ are also shown in Fig. 1. The constraints (3.10) and (3.11) may be considered as eight linear equations or

sum rules for ten unknowns $P(^{18}v, {}^{16}v)$, i.e., the given experimental information on $^{16}P_{expt}(^{16}v)$, $^{18}P_{expt}(^{18}v)$ restricts the possible $P(^{18}v, {}^{16}v)$ to an only $10-8=2$-dimensional manifold. Explicitly, the noted absence of highly excited product radicals $^{16}OH(^{16}v=3)$, $^{18}OH(^{18}v=2)$ and $^{18}OH(^{18}v=3)$ implies [via Eqs. (3.10), (3.11)] that

$$P(^{18}v=0, {}^{16}v=3) = P(^{18}v=2, {}^{16}v=0)$$

$$= P(^{18}v=2, {}^{16}v=1) = P(^{18}v=3, {}^{16}v=0) = 0 \ . \qquad (3.14)$$

Furthermore, let us denote

$$P(^{18}v=1, {}^{16}v=1) = \delta \ , \qquad (3.15)$$

$$P(^{18}v=1, {}^{16}v=2) = \epsilon \ . \qquad (3.16)$$

Then, using the experimental values of $^{16}P_{expt}(^{16}v)$ and $^{18}P_{expt}(^{18}v)$, the point vibrational probability matrix $P(^{18}v, {}^{16}v)$ may be expressed as

$$\begin{matrix} \uparrow \\ {}^{18}v \end{matrix} \begin{pmatrix} 0 & - & - & - \\ 0 & 0 & - & - \\ 0.046-\delta-\epsilon & \delta & \epsilon & - \\ 0.450+\delta+\epsilon & 0.340-\delta & 0.164-\epsilon & 0 \end{pmatrix} . \qquad (3.17)$$
$$\qquad\qquad {}^{16}v \rightarrow$$

Here $P(^{18}v, {}^{16}v)$ is written such that the row index increases with ^{18}v from bottom to top, in analogy with Fig. 1. The dashes indicate energetically inaccessible level combinations, as explained in Sec. III A. The zeros denote vanishing probability matrix elements, as implied by the sum rules [cf. Eq. (3.14)] and the ϵ and δ clearly indicate the anticipated mathematical two-dimensional variability of $P(^{18}v, {}^{16}v)$. By summing rows and columns of $P(^{18}v, {}^{16}v)$ one readily verifies the sum rules (3.10) and (3.11) as well as the normalization of $P(^{18}v, {}^{16}v)$. One can even go one step further and exploit the nonnegativity of probabilities. This imposes three inequality constraints on ϵ and δ namely,

$$0 \le \epsilon, \quad 0 \le \delta, \quad \delta + \epsilon \le 0.046 \ . \qquad (3.18)$$

As can be readily concluded from expressions (3.17) and (3.18), the energy conservation together with the experimental vibrational product distributions of $^{16}OH(^{16}v)$ and $^{18}OH(^{18}v)$ already determine the joint probabilities $P(^{16}v, {}^{16}v)$ within rather narrow limits (± 0.02). What remains unknown at this level are the precise values of ϵ and δ. One possible realization is $(\epsilon, \delta) \simeq (0, 0)$ i.e., pairs of vibrationally excited hydroxyls are improbable, [cf. Eqs. (3.15), (3.16)]. This case is illustrated schematically by contour lines in the triangle plot of Fig. 1. However, quite different realizations are possible as well, e.g., $(\delta, \epsilon) \simeq (0, 0.046)$. In this case $^{18}OH(^{18}v=1)$ might be created preferably with its partner $^{16}OH(^{16}v=2)$ excited to $^{16}v=2$. In order to determine (δ, ϵ) more precisely, we shall invoke information theory and exploit the whole experimental information on $^{18}P(^{18}f)$ and $^{16}P(^{16}f)$ instead of only $^{18}P(^{18}v)$ and $^{16}P(^{16}v)$. As we shall see, the experimental rotational hydroxyl radical distributions will imply that the first guess $(\delta, \epsilon) \simeq (0, 0)$ is essentially correct.

C. Surprisal synthesis

Experiment provides us with the measured internal probability distributions $P_{expt}(f)$ of both product radicals of the title reaction. Altogether, there are about 120 individual data points for the various combinations of quantum numbers $f = (j, \Omega, v)$ for both isotopes. When these data are inserted into the left-hand sides of Eqs. (1.2) and (1.3), we obtain correspondingly 120 sum rules as constraints on the $\simeq 8000$ joint probabilities $P(^{18}f, {}^{16}f)$. Just as explained in Sec. III B for the vibrational manifolds, these 120 constraints impose considerable limits on the possible values of $P(^{18}f, {}^{16}f)$ but do not suffice for their unique specification. Information theory[10] fills the gap by the requirement that the optimum $P(^{18}f, {}^{16}f)$ should satisfy all constraints (sum rules) and be otherwise as statistical as possible. Thus the theoretical $P(^{18}f, {}^{16}f)$ is obtained by maximizing the entropy, or equivalently, minimizing the information

$$\Delta S[(^{18}f, {}^{16}f)] = R \sum_{^{18}f} \sum_{^{16}f} P(^{18}f, {}^{16}f) \times \ln[P(^{18}f, {}^{16}f)/P^0(^{18}f, {}^{16}f)] \ , \qquad (3.19)$$

subject to the constraints (1.2) and (1.3). In this way it is possible, in principle, to predict the least biased joint distribution $P(^{18}f, {}^{16}f)$ that is compatible with the experimental results $^{16}P_{expt}(^{16}f)$ and $^{18}P_{expt}(^{18}f)$. The probabilities P^0 in Eq. (3.19) are the information theoretic prior distributions; they are proportional to the degeneracy of the joint levels $(^{18}f, {}^{16}f)$.[10]

The solution of Eqs. (3.19), (1.2), (1.3) is obtained with the help of Lagrangian parameters as

$$P(^{18}f, {}^{16}f) = P^0(^{18}f, {}^{16}f) \times \exp\left[-\lambda_0 - \sum_{^{16}\tilde{f}} \lambda(^{16}\tilde{f})\,\delta(^{16}\tilde{f}, {}^{16}f) - \sum_{^{18}\tilde{f}} \lambda(^{18}\tilde{f})\delta(^{18}\tilde{f}, {}^{18}f)\right] . \qquad (3.20)$$

In Eq. (3.20) the sums are over all available levels, and the Kronecker-type $\delta(\tilde{f}, f)$ is equal to unity if level f occurs in the experimental sum rule for $P(\tilde{f})$; else it vanishes. The λ_0 is a normalization constant.

The route of Eq. (3.20) is called "surprisal synthesis", and is complementary to the surprisal analysis of the title reaction.[4] However, while the surprisal synthesis yields, in principle, proper results, they would not be very satisfactory for the present purpose. The reason is that the number of Lagrangian parameters equals the number of sum rules plus one, i.e., it is $\simeq 120$! Such a large number of parameters raises immediate questions of their sensitivity, not to mention their numerical evaluation, and above all it clearly tends to screen the physics of reaction. What we prefer is a clear model which reproduces approximately the experimental results with a much smaller number of parameters. This is the alternative "route of persuasion"[10] of the information theoretic approach, which we shall pursue in Sec. III E. But first we develop a simple model for the reaction (1.1).

TABLE I. Maximum rotational levels j_{max} of OH radicals within vibrational manifold v.

	Experiment		Theory using conservation of	
v	^{18}OH	^{16}OH	energy[a] + angular momentum[b]	only energy[a]
0	18.5[c]	22.5[c,d]	18.5	26.5
1	8.5[e]	15.5[c]	15.5	22.5
2	...	9.5	11.5	17.5

[a]Using the average value (3.5) for $E = 147.5$ kJ mol^{-1} in Eq. (3.6). Slightly higher (+1, +2) maximum values for j_{max} arise from the maximum value $E_{max} = 154.2$ kJ mol^{-1} (see Appendix A).
[b]Using Eqs. (3.24) and (3.26).
[c]The value 17.5 is reported in Ref. 8.
[d]There is indirect evidence for the value 23.5 in Fig. 2 of Ref. 9.
[e]The value 14.5 is read from Fig. 8 of Ref. 8. In the present work, higher j levels are difficult to detect due to the small fraction $^{18}P(^{18}v = 1) = 0.046$.

D. Angular momentum transfer

The total angular momentum J of the title reaction may be written as a conserved quantity for reactants and products,

$$\mathbf{j}[^{16}O(^1D)] + \mathbf{j}(H_2{}^{18}O) + \mathbf{l} = \mathbf{J} = \mathbf{j}(^{16}OH) + \mathbf{j}(^{18}OH) + \mathbf{l}' , \quad (3.21)$$

where $\mathbf{j}$ and $\mathbf{l}$ denote rotational and orbital angular momenta, respectively. In the present situation, $j[^{16}O(^1D)] = 2\hbar$, $j(H_2{}^{18}O) \simeq (2-3)\hbar$ for $H_2{}^{18}O$ at $T = 300$ K, and an average value of $l \simeq 26\ \hbar$ is estimated from the absolute value of the rate coefficient[5] (see Appendix B). Moreover, the title reaction is a light-atom transfer reaction. Kinematic constraints together with the relation

$$l \gg j[^{16}O(^1D)],\ j(H_2{}^{18}O) , \quad (3.22)$$

then imply (see Ref. 33) that initial orbital angular momentum is essentially transferred into final orbital angular momentum,

$$\mathbf{l} \simeq \mathbf{J} \simeq \mathbf{l}' . \quad (3.23)$$

Relation (3.23) may be interpreted as follows: initially, the relative motion of the heavy ^{16}O and ^{18}O atoms is the dominant source of total angular momentum. This orbital momentum remains stored in the heavy atoms and is only marginally influenced by the light atom transfer during reaction. As a consequence of relations (3.21)–(3.23),

$$\mathbf{j}(^{16}OH) \simeq -\mathbf{j}(^{18}OH) , \quad (3.24)$$

i.e., both radicals rotate with opposite angular velocity such that the total rotational orbital momentum of the product pair nearly vanishes (in comparison with the orbital angular momenta). There is some indirect experimental evidence for relation (3.24), namely, the average rotational fractions $\langle f_R \rangle = \bar{E}_{rot}/E$ of energy E for both hydroxyl radicals are small and about equal,

$$\langle f_R(^{18}OH) \rangle = 0.058 \simeq \langle f_R(^{16}OH) \rangle = 0.067 . \quad (3.25)$$

Furthermore, this near equality even holds for the individual rotational levels (summed over all vibrational states[4]). A third item of evidence will be discussed later in connection with Table I. Therefore, we now make the simplifying model assumption that Eq. (3.24) holds exactly. While Eq. (3.25) tells us that this model assumption is only approximate, the kinematic considerations imply that it should be essentially correct. We thus sacrifice the rigor of the surprisal synthesis, Sec. III C, at the expense of the physical insight provided by the model (3.24) to be used in the route of persuasion, Sec. III E. We anticipate the relative error in Eq. (3.24) should be largest for the smallest absolute values of $j = 1/2$, $3/2$, and $5/2$, due to the effects of the initial rotational angular momenta; i.e., the theoretical results for small values of j will underestimate the exact ones.

An immediate consequence of the rigorous model assumption (3.24) is that all joint probabilities $P(^{18}f, {}^{16}f)$ should vanish unless the products' rotational angular momenta are (approximately) identical

$$P(^{18}j, {}^{18}\Omega, {}^{18}v, {}^{16}j, {}^{16}\Omega, {}^{16}v) \simeq 0 \quad \text{for } {}^{18}j \neq {}^{16}j . \quad (3.26)$$

Equation (3.26) together with the energy conservation of Eq. (3.6) considerably reduces the range of accessible rotational energy levels in a given vibrational manifold of the product hydroxyl radicals. On purely energetic grounds, it would be possible that one hydroxyl radical is rotationally cold, whereas the other accumulates all the remaining available energy in rotational motion. In contrast, the model requires that the nonvibrational part of the available energy must be shared between the pair of product radicals approximately according to Eq. (3.26). The resulting maximum values of j are listed in Table I, together with the maximum observed experimental j's. It is gratifying that the experimental values are usually below the upper bounds implied by Eqs. (3.6) and (3.26). The one exceptional case is well within the error limits ($\simeq +4$) implied by the transfer of reactant rotational angular momentum which is neglected in the simple model. Altogether there are six experimental data points (out of 121) with very low (< 0.003) probabilities which fall into this range of very high rotational motion; these are neglected in the analysis in Sec. IV. In conclusion, we consider the consistency of Table I as further evidence for the validity of the model, Eq. (3.26).

Another consequence of the near collinearity of the product angular momenta equations (3.24) is that the rotational levels of the hydroxyl radical pairs are only $\simeq (2j+1)$ fold degenerate, not $(2\,{}^{16}j + 1) \times (2\,{}^{18}j + 1)$ fold. Therefore, the appropriate prior probability for the coincident events is

$$P^0(^{18}j = j,\ {}^{18}\Omega,\ {}^{18}v,\ {}^{16}j = j,\ {}^{16}\Omega,\ {}^{16}v) = N(2j+1)E_{trans}^{1/2} , \quad (3.27)$$

where N is a normalization constant, and $E_{trans}^{1/2}$ measures the translational degeneracy.[10]

It should be noted that the constraint (3.24) does not allow an approximate kinematic predetermination of the product rotational distribution. This is in marked contrast with the situation of atom–diatom reactions (see Refs. 33–35). All that we wish to adapt from diatomic experience is the assumption of a dynamical constraint which rules the average rotational fraction $\langle g_R(^{18}v, {}^{16}v) \rangle$ of the nonvibrational energy $E - {}^{18}E(^{18}v) - {}^{16}E(^{16}v)$ for the

emerging *pair* of products $^{18}OH(^{18}v)$ and $^{16}OH(^{16}v)$,

$$\langle g_R(^{18}v, {}^{16}v)\rangle = \sum_{^{18}j} \sum_{^{18}\Omega=1/2}^{3/2} \sum_{^{16}j} \sum_{^{16}\Omega=1/2}^{3/2} P(^{18}f, {}^{16}f) \cdot g_R(^{18}f, {}^{16}f; {}^{18}v, {}^{16}v), \tag{3.28}$$

where

$$g_R(^{18}f, {}^{16}f; {}^{18}v, {}^{16}v) = \frac{{}^{18}E(^{18}f) + {}^{16}E(^{16}f) - {}^{18}E(^{18}v) - {}^{16}E(^{16}v)}{E - {}^{18}E(^{18}v) - {}^{16}E(^{16}v)} . \tag{3.29}$$

The constraint on $\langle g_R(^{18}v, {}^{16}v)\rangle$ expresses that any reactive encounter populating the levels $(^{18}v, {}^{16}v)$ will distribute a certain amount of remaining energy simultaneously and not independently among the rotational degrees of freedom of both products, without specifying the mechanism explicitly.

E. Persuasion

Let us assume for the moment that the predetermined values of $\langle g_R(^{18}v, {}^{16}v)\rangle$ were available, either experimentally or by a theoretical model. Then Eq. (3.28) together with the sum rules (3.10) and (3.11) should be used as constraints in the surprisal synthesis that minimizes Eq. (3.19). Taking into account the angular momentum transfer by Eqs. (3.26) and (3.27), the resulting joint probabilities may be written as

$$P_{\text{theor}}(^{18}j, {}^{18}\Omega, {}^{18}v, {}^{16}j, {}^{16}\Omega, {}^{16}v) = P(^{18}j, {}^{18}\Omega, {}^{16}j, {}^{16}\Omega \,|\, {}^{18}v, {}^{16}v) P(^{18}v, {}^{16}v) , \tag{3.30}$$

(the subscript "theor" means "theoretical") where $P(^{18}v, {}^{16}v)$ are the joint vibrational probabilities (3.17) and $P(^{18}j, {}^{18}\Omega, {}^{16}j, {}^{16}\Omega \,|\, {}^{18}v, {}^{16}v)$ are the conditional probabilities of observing rotational and electronic quantum numbers $(^{18}j, {}^{18}\Omega, {}^{16}j, {}^{16}\Omega)$ given that the pair of hydroxyls is formed with vibrational quantum numbers $(^{18}v, {}^{16}v)$. From Eq. (3.26) it follows that

$$P(^{18}j, {}^{18}\Omega, {}^{16}j, {}^{16}\Omega \,|\, {}^{18}v, {}^{16}v) = 0 , \quad \text{for } {}^{18}j \neq {}^{16}j , \tag{3.31}$$

whereas for equal $^{18}j = {}^{16}j = j$, the surprisal synthesis yields

$$P(^{18}j = j, {}^{18}\Omega, {}^{16}j = j, {}^{16}\Omega \,|\, {}^{18}v, {}^{16}v) = N(^{18}v, {}^{16}v)(2j+1)E_{\text{trans}}^{1/2} \times \exp[-\Theta(^{18}v, {}^{16}v) g_R(^{18}f, {}^{16}f; {}^{18}v, {}^{16}v)] . \tag{3.32}$$

The $N(^{18}v, {}^{16}v)$ are normalization constants, $(2j+1)E_{\text{trans}}^{1/2}$ represents the prior (3.27), and the last factor contains the surprisal arising from the constraint on $g_R(^{18}v, {}^{16}v)$, Eq. (3.28). Note that we have explicitly written $(^{18}v, {}^{16}v)$-dependent surprisal parameters Θ, because the empirical v independence of Θ which is usually found for atom–diatom collisions[10,36,37] must not necessarily hold in the case of two diatomic products. One might suppose that in a more coherent presentation the $P(^{18}v, {}^{16}v)$ should have been expressed also using surprisal parameters, but we prefer the form (3.17) primarily since it accounts for the eight sum rules (3.10) and (3.11) with the minimum number (=2) of parameters, δ and ϵ [see Eqs. (3.15) and (3.16)]. A more fundamental reason for using Eq. (3.17) will become evident in Sec. IV. From Eq. (3.14) it follows that Eq. (3.32) must be evaluated only for the nonvanishing combinations where $^{16}v = 0, 1$ or 2 and $^{18}v = 0, 1$. In conclusion, there are eight parameters δ, ϵ, and six $\Theta(^{18}v, {}^{16}v)$'s to reproduce 115 experimental data $^{16}P_{\text{expt}}(^{18}f)$, $^{16}P_{\text{expt}}(^{16}f)$ using the present model. Notice, however, that we cannot determine these parameters *a priori*, since the assumed values for $\langle g_R(^{18}v, {}^{16}v)\rangle$ are actually unknown. Nevertheless, we may predict the theoretical form obeyed by the product radicals' internal distributions, namely,

$${}^{16}P_{\text{theor}}(^{16}f) = \sum_{^{18}f} P_{\text{theor}}(^{18}f, {}^{16}f) , \tag{3.33}$$

$${}^{18}P_{\text{theor}}(^{18}f) = \sum_{^{16}f} P_{\text{theor}}(^{18}f, {}^{16}f) , \tag{3.34}$$

where $P_{\text{theor}}(^{18}f, {}^{16}f)$ is given by Eqs. (3.30)–(3.32), in analogy with Eqs. (3.10) and (3.11).

Information theory suggests[10] that in a final step, the unknown parameters ϵ, δ, and $\Theta(^{18}v, {}^{16}v)$ should now be determined by fitting the theoretical probabilities (3.33) and (3.34) to the experimental data. Explicitly, the persuasion[10]

$$2H = \sum_{^{18}f} {}^{18}P_{\text{expt}}(^{18}f) \ln[{}^{18}P_{\text{expt}}(^{18}f)/{}^{18}P_{\text{theor}}(^{18}f)] + \sum_{^{16}f} {}^{16}P_{\text{expt}}(^{16}f) \ln[{}^{16}P_{\text{expt}}(^{16}f)/{}^{16}P_{\text{theor}}(^{16}f)] \tag{3.35}$$

should be minimized (we have included an irrelevant factor 2 since the internal probabilities of $^{18}OH(^{18}f)$ and $^{16}OH(^{16}f)$ are normalized independently). The sums in Eq. (3.35) are over all levels ^{18}f, ^{16}f that have been measured experimentally. When H is minimized, the information contents of the experimental and theoretical probabilities are as similar as possible.[10] The results are presented in Sec. IV.

IV. RESULTS AND DISCUSSION

A. Vibrational distribution

The experimental and theoretical model information presented in Sec. III yields the following joint vibrational probability matrix:

$$P(^{18}v, {}^{16}v) = \begin{pmatrix} 0 & - & - & - \\ 0 & 0 & - & - \\ 0.044 & 0.002_3 & 0 & - \\ 0.452 & 0.338 & 0.164 & 0 \end{pmatrix} . \tag{4.1}$$

Comparison with Eq. (3.17) shows that the parameters $(\delta, \epsilon) \simeq (0.002_3, 0)$. The result (4.1) has been plotted qualitatively as contours in the triangle plot of Fig. 1. It has important consequences concerning the mechanism of the elementary reaction, the interpretation of the data, and the theory, as explained below.

The fact that $\epsilon = P(^{18}v = 1, {}^{16}v = 2)$ vanishes within numerical accuracy means that the reaction must be very direct; a collision complex which shares energy between the vibrational levels of both radicals is *completely* ruled out. The same conclusion arises within the limits

of the very small value $\delta = P(^{18}v=1,\ ^{16}v=1) = 0.002_3$. Apparently either the "new" radical ^{16}OH is vibrationally excited in an encounter, or, to a much smaller extent, the "old" radical ^{18}OH, but not both simultaneously. Summation of the rows and columns of the probability matrix (4.1) yields the experimental vibrational distributions of ^{18}OH and ^{16}OH, as illustrated in Fig. 1. However, the matrix (4.1) now tells us much more. For example, the observed distribution of ^{18}OH in the vibrational ground state is actually a superposition of three distinct events leaving the collision partner $^{16}OH(^{16}v)$ in levels $^{16}v=0, 1$ or 2. The other extreme is the observed distribution of $^{16}OH(^{16}v=2)$ which is definitely "clean," i.e., it arises exclusively from pair events with $^{18}OH(^{18}v=0)$. The other three cases are intermediate between these two extreme cases, with $^{16}OH(^{16}v=1)$ and $^{18}OH(^{18}v=1)$ being practically "clean" [since $\delta = 0.002_3$, cf. Eq. (4.1)], whereas the $^{16}OH(^{16}v=0)$ distribution should be a superposition with substantial contributions from product partners $^{18}OH(^{18}v=0)$ and $^{18}OH(^{18}v=1)$.

On the theoretical side, the case $\epsilon = 0$ is remarkable. Firstly, it implies that a constraint on $\langle g_R(^{16}v=2,\ ^{18}v=1)\rangle$ cannot be informative, so that we lose $\Theta_R(^{18}v=2,\ ^{18}v=1)$ as a parameter, i.e., the 115 data are actually fitted by only seven parameters. Secondly, the case $\epsilon = 0$ is exceptional—in fact, the first nontrivial practical case we know of—as it means that the convex persuasion function H, Eq. (3.35) attains its minimum value on the boundary of its domain. In this case, the method of Lagrangian multipliers may not be optimal, and this is the deeper reason why we have used the alternative (3.17) in Sec. III.[38]

B. Rotational distributions

The rotational distributions (3.32) are determined by optimal suprisal parameters $\Theta(^{18}v,\ ^{16}v)$ which are presented in matrix form analogous to the joint probability matrix $P(^{18}v,\ ^{16}v)$:

$$\Theta(^{18}v,\ ^{16}v) = \begin{pmatrix} - & - & - & - \\ - & - & - & - \\ 16.0 & -0.1 & - & - \\ 4.0 & 6.9 & 9.4 & - \end{pmatrix} \begin{matrix} \\ \\ \\ \uparrow \\ {}^{18}v \end{matrix} \cdot \qquad (4.2)$$

$$^{16}v \rightarrow$$

The dashes in Eq. (4.2) indicate that the corresponding $P(^{18}v, ^{16}v)$ vanishes, i.e., $\Theta(^{18}v, ^{16}v)$ does not exist. The corresponding five joint-rotational distributions of the $^{18}OH(^{18}v) + {}^{16}OH(^{16}v)$ pairs, summed over the electronic quantum numbers

$$P(^{18}j=j,\ ^{18}v,\ ^{16}j=j,\ ^{16}v) = \sum_{^{18}\Omega=1/2} \sum_{^{16}\Omega=1/2} P(^{18}f,\ ^{16}f)\,, \qquad (4.3)$$

are shown in Fig. 2 vs j, the absolute value of the opposite internal rotational angular momenta of the radicals (3.24).

Also indicated in Fig. 2 are the maximum values j_{max} of j for each $(^{18}v, ^{16}v)$ manifold, as implied by energy and angular momentum transfer constraints, cf. Eqs.

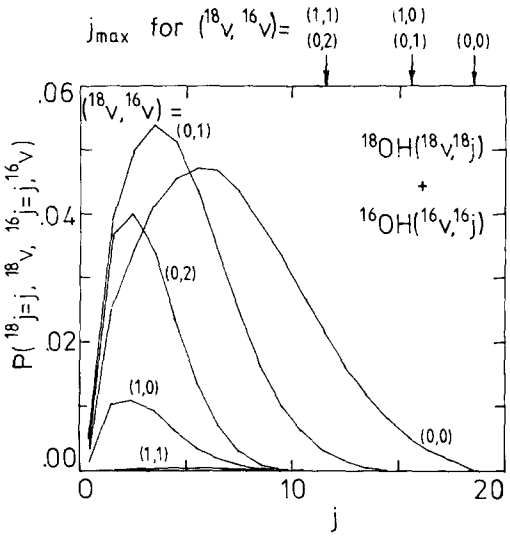

FIG. 2. Joint rovibrational probabilities $P(^{18}j=j,\ ^{18}v,\ ^{16}j=j,\ ^{16}v)$ vs angular momentum j for the five vibrational pairs $(^{18}v,\ ^{16}v)$ of the reaction $^{16}O(^1D) + H_2\,^{18}O \rightarrow {}^{18}OH(^{18}j,\ ^{18}v) + {}^{16}OH(^{16}j,\ ^{16}v)$. The upper limits j_{max} of j, arising from energy and angular momentum constraints, are indicated on the top for each $(^{18}v,\ ^{16}v)$ pair.

(3.6) and (3.26). As is evident from Fig. 2 and expressions (4.2) and (3.32), the rotational distributions are Boltzmann-type, and in general the rule holds: the higher a radical pair's vibrational excitation, the less its rotational one, i.e., *the rotational distributions "die out" before reaching their upper limits* j_{max}.

There is, however, one remarkable exception to this rule: The $(^{18}v=1,\ ^{16}v=1)$ case, where $\Theta_R(1,1) = -0.1$, i.e., the rotational distribution is nearly statistical and extends up to its maximum value $j_{max}(1,1) = 11.5$. We wish to emphasize that this result is certain even though the precise value of $\Theta_R(1,1)$ is the most sensitive of all parameters, due to the smallness of $P(^{18}v=1,\ ^{16}v=1)$. It thus appears that the extremely rare encounters that lead to two vibrationally excited radicals also favor their rotational excitation. Conversely, the larger is the energy disposal into the vibrational mode of one radical (leaving the other one cold), the more hindered is the rotational excitation.

C. Internal distributions

The internal distributions $P_{theor}(f)$ are obtained by summing the joint distributions $P(^{18}f,\ ^{16}f)$ illustrated in Fig. 2, cf. Eqs. (3.33) and (3.34). The fully state resolved results are plotted vs j in Fig. 3. Also included are the experimental results $P_{expt}(f)$ for direct comparison with the theoretical results. In order to judge the agreement obtained, one should also consider the experimental error limits (Sec. II) and notice the linear scales of the ordinates. On logarithmic scales with the P's divided by the rotational degeneracy factors $(2j+1)$, see Refs. 4 and 8, the agreement would have appeared better. Instead of pointing to the satisfactory overall agreement of the theoretical and experimental distributions, below we shall more strongly emphasize the re-

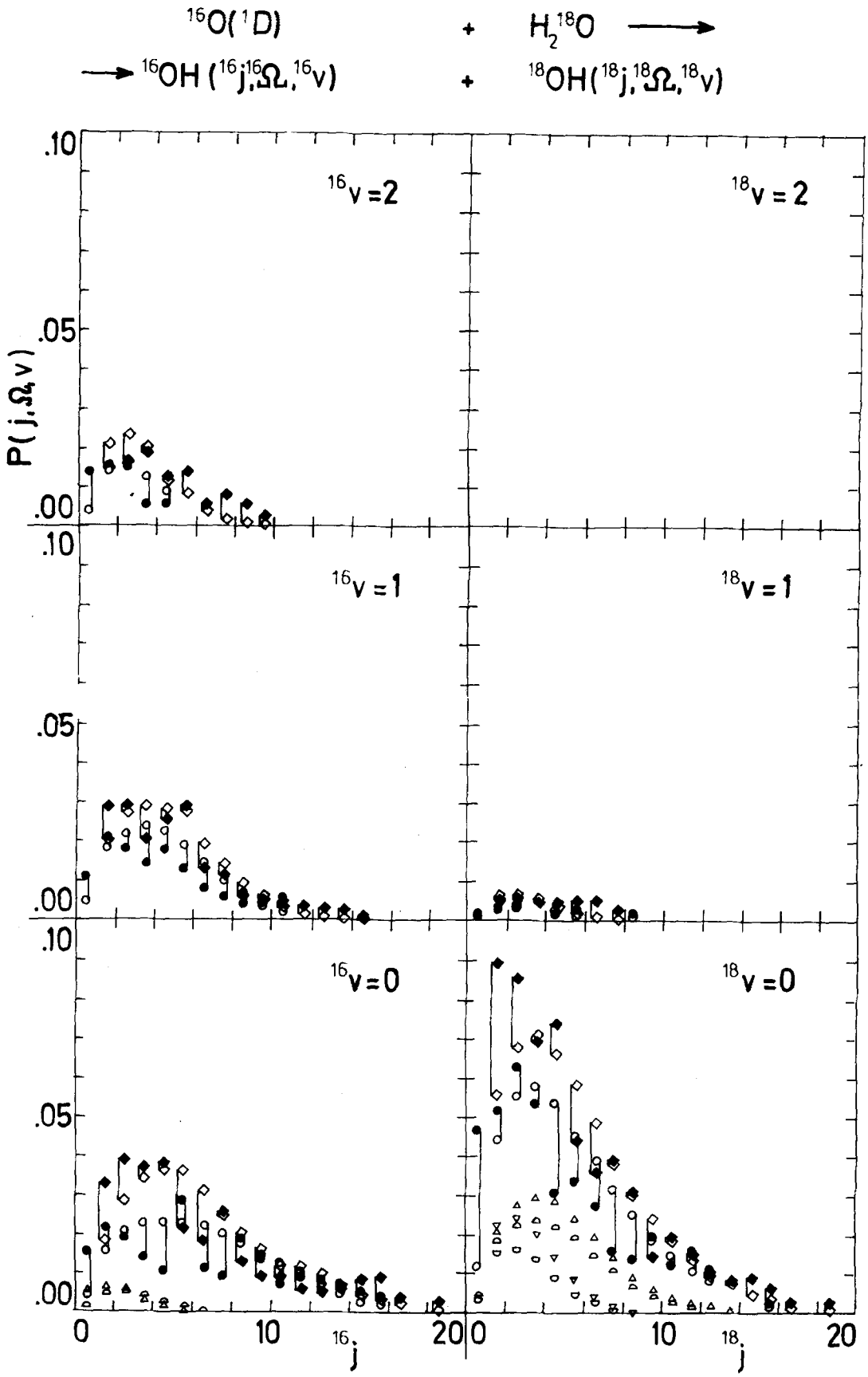

FIG. 3. Experimental (filled symbols) and theoretical (open symbols) probabilities $P(j, \Omega, v)$ for the populations of internal levels of the product radicals of the $^{16}O(^1D) + H_2{}^{18}O \rightarrow {}^{16}OH(^{16}j, {}^{16}\Omega, {}^{16}v) + {}^{18}OH(^{18}j, {}^{18}\Omega, {}^{18}v)$ reaction vs j. Circles and squares devote $\Omega = 1/2$ and $3/2$, respectively. Most radicals arise with the partners in the vibrational ground state $v = 0$. Significant contributions from collisions populating the partners vibrational level $v = 1$ and 2 are indicated by symbols ⌓ ($\Omega = 1/2$), Δ ($\Omega = 3/2$) and ⌔ ($\Omega = 1/2$), ∇($\Omega = 3/2$), respectively. For convenient comparison equivalent experimental and theoretical data are connected by vertical bars.

maining discrepancies. The two most important ones are:

(a) The theoretical distributions are in general much more smooth than the experimental ones. This may be due, in part, to the simple model used and to the experimental error limits, as discussed in Sec. II.

(b) The low-j-experimental P_{expt}'s are usually larger than the corresponding theoretical P_{theor}'s. This result has been anticipated in Sec. III as a consequence of relatively large deviation from the law (3.24) for low values of j. In addition, relaxation effects tend to repopulate the experimental low-j P's.[4,8,9]. Removing this possible artifact would improve in general the overall agreement of all experimental and theoretical P's.

Having discussed the quality of theoretical and experimental results, we close this section with an important conclusion which will hold irrespective of the indicated theoretical and experimental refinements: As explained in Sec. IV A, the observed distributions for $^{18}OH(^{18}v=0)$ and $^{16}OH(^{16}v=0)$ arise actually from superpositions of joint reaction probabilities with the partner hydroxyls each in several vibrational levels, respectively. These contributions are also indicated in Fig. 3. In contrast, the $^{18}OH(^{18}v=1)$, $^{16}OH(^{16}v=1)$, and $^{16}OH(^{16}v=2)$ distributions are essentially or even rigorously clean, i.e., they arise from collisions yielding the product partner in the vibrational ground state. As a consequence, *only* the plotted theoretical $^{18}OH(^{18}v=1)$, $^{16}OH(^{16}v=1)$ and $^{16}OH(^{16}v=2)$ are characterized, in practice, by single surprisal parameters $\Theta_R(^{18}v=1, {}^{16}v=0)$, $\Theta_R(^{18}v=0, {}^{16}v=1)$, and $\Theta_R(^{18}v=0, {}^{16}v=0)$, respectively, cf. Eq. (4.2).

The corresponding "rotational temperatures" are 790, 1820, and 820 K, which should be compared with the values 1200, 1600, and 600 K of Ref. 4. The differences are mainly due to a tentative account of relaxation phenomena in Ref. 4 and to the different priors used in Ref. 4 and in the present work.

V. CONCLUSIONS

The method presented in this paper for obtaining joint microscopic reaction probabilities from experimental internal product states offers two routes which should be applicable to quite arbitrary reactions of the type $A + BCD \rightarrow AB(^{AB}f) + CD(^{CD}f)$. The first one is surprisal synthesis where the $P(^{AB}f, {}^{CD}f)$ are obtained using pure sum rule constaints on the experimental distributions $^{AB}P(^{AB}f)$ and $^{CD}P(^{CD}f)$. The other one is the route of persuasion. It requires a model for the reaction which may then be tested by comparison of the theoretical and experimental $^{AB}P(^{AB}f)$ and $^{CD}P(^{CD}f)$. The first route is preferable if one aims at the least-biased results. The second route allows one to gain insight into the physics of reaction. This route has been exemplified here. In general, the techniques used are straightforward extensions of the information theoretic approach to reactions yielding atomic plus molecular products with state resolved internal distributions of the one molecule.[10]

The reaction $^{16}O(^1D) + H_2{}^{18}O \rightarrow {}^{16}OH(^{16}f) + {}^{18}OH(^{18}f)$ may be considered as a particularly "lucky case" for the determination of joint probabilities $P(^{16}f, {}^{18}f)$ for several reasons:

(a) it is the system with the most detailed experimental information on the products' internal distributions[3,4], [compare with the pioneering results of Smith on the $O(^3P) + CS_2 \rightarrow SO + CS$ reaction.[30]]

(b) The vibrational energy disposal is very specific (see the triangle plot, Fig. 1). As a consequence, the entire vibrational probability matrix $P(^{18}v, {}^{16}v)$ for observing $^{18}OH(^{18}v) + {}^{16}OH(^{16}v)$ coincident pairs is determined within narrow limits (± 0.02) from the experimental $^{18}P_{expt}(^{18}v)$ and $^{16}P_{expt}(^{16}v)$ via sum rule constraints, *without* using additional model assumptions or information theory.

(c) The mass ratios and initial values of angular momenta allow use of a simple kinematic model which essentially further constrains the joint rotational $(^{18}j, {}^{16}j)$ manifold to the diagonal $^{18}j \simeq {}^{16}j \simeq j$. As a consequence of (a)–(c), we are able to reproduce semiquantitatively the ~120 experimental data of internal product populations with seven parameters, cf., Fig. 3. Altogether, these seven parameters account for ≈ 8000 distinct coincident pair events, thus providing an other example of an enormous semiquantitative compaction of data by information theory, see Ref. 10. The results allow several specific conclusions to be drawn about the reaction dynamics of the title system.

(d) The internal and electronic angular momentum distributions of the excited vibrational manifolds of one product radical arise from collisions which leave the partner radical in its vibrational ground state. Furthermore, the corresponding rotational surprisal parameters have large positive values. This means that for $^{16}v \neq 0$ or $^{18}v \neq 0$, energy disposal in the remaining internal degrees of freedom is quite specific.

(e) As a consequence of (d) it is clear that the reaction is very direct. It must proceed on a time scale which does not allow for efficient energy transfer into all the available phase space. One possible origin for such a specific energy release may be that the reaction proceeds via a rather specific collision geometry.

(f) Conversely, the internal distributions of vibrationally cold ^{16}OH and ^{18}OH arise from collisions leaving the partners excited into several vibrational levels. Via angular momentum constraints, the observed distribution of the vibrationally excited OH radicals (see the top and center of Fig. 3) also contribute to the internal distributions of their $v=0$ partners (marked by symbols Δ, ∇, $\frown$, $\smile$, in the bottom panel of Fig. 3). Therefore it does not seem reasonable to represent the unrelaxed $v=0$ distributions by a single rotational surprisal (or temperature[3,8,9]) parameter.

(g) As a consequence of (f), it appears to be more difficult to extrapolate post-collisional relaxation effects from semilogarithmic probability plots than expected.

(h) Theory predicts the complete absence of encounters leading to $^{16}OH(^{16}v=2) + {}^{18}OH(^{18}v=1)$ coincident pairs. An experiment is currently being done to test this prediction. The idea is to employ translationally cold reac-

tants such that the ($^{18}v = 1$, $^{16}v = 2$) channel is energetically closed. Any possible contributions to ($^{18}v = 1$, $^{16}v = 2$) in the present experiment would then lead to considerable changes in the $^{16}v = 2$ distribution.

In conclusion, the insight gained into the title reaction appears to be considerable, and provides stimulating ideas for future research.

ACKNOWLEDGMENT

We should like to thank Dr. J. E. Butler for sending us a preprint of his paper prior to publication. J. M. also thanks Professor R. D. Levine for discussions in connection with inequality constraints. Financial support by the Deutsche Forschungsgemeinschaft and the Fonds der Chemischen Industrie are gratefully acknowledged. The computations have been carried out on the CYBER 175 of the Bayerische Akademie der Wissenschaften.

APPENDIX A: TRANSLATIONAL REACTION ENERGY

The velocities of reactants $H_2{}^{18}O$ and $^{16}O(^1D)$, where $^{16}O(^1D)$ arises from O_3 dissociation, are illustrated schematically in Fig. 4. The translational energy of reactants is

$$E_{\text{trans}} = \tfrac{1}{2}\mu_{O,H_2O}\overline{\mathbf{v}^2_{O,H_2O}} , \tag{A1}$$

where μ_{O,H_2O} is the reduced mass of $^{16}O + H_2{}^{18}O$. Using Fig. 4 it follows that

$$\mathbf{v}_{O,H_2O} = -\mathbf{v}_{O_3} - \mathbf{v}_{O\,c.m.} + \mathbf{v}_{H_2O} , \tag{A2}$$

with $\mathbf{v}_{O\,c.m.}$ the ^{16}O velocity in the O_3 center-of-mass system. Explicitly,

$$\mathbf{v}_{O\,c.m.} = \mathbf{v}_{O,O_2}[m_{O_2}/(m_{O_2} + m_O)] , \tag{A3}$$

where $\mathbf{v}_{O,O_2}$ is the relative velocity of the dissociated $^{16}O + {}^{16}O_2$. In the present experiment all velocities are oriented randomly. Therefore, inserting Eqs. (A2) and (A3) into Eq. (A1) and carrying out the velocity average indicated by the bar, we obtain:

$$\overline{v^2_{O,H_2O}} = \overline{v^2_{H_2O}} + \overline{v^2_{O_3}} + \overline{v^2_{O,O_2}}[m_{O_2}/(m_{O_2} + m_O)]^2 . \tag{A4}$$

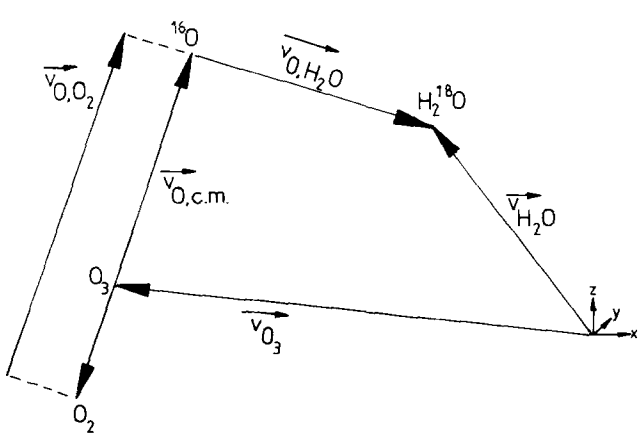

FIG. 4. The velocities of reactants $H_2{}^{18}O$ and ^{16}O where ^{16}O originates from O_3 dissociation.

The averages on the right-hand side of Eq. (A4) are estimated from the relations

$$\tfrac{1}{2}m_{H_2O}\overline{v^2_{H_2O}} = \tfrac{3}{2}\,RT \tag{A5}$$

and

$$\tfrac{1}{2}m_{O_3}\overline{\mathbf{v}^2_{O_3}} = \tfrac{3}{2}\,RT , \tag{A6}$$

for thermal distributions of $H_2{}^{18}O$ and $^{16}O_3$, respectively. Furthermore,

$$\tfrac{1}{2}\mu_{O,O_2}v^2_{O,O_2} = E_{\text{trans}\,O,O_2} , \tag{A7}$$

where $E_{\text{trans}\,O,O_2}$ and μ_{O,O_2} are the translational energy and reduced mass of the dissociated $^{16}O + {}^{16}O_2$, respectively. $E_{\text{trans}\,O,O_2}$ has a nonthermal distribution that has been determined experimentally.[31] The dominant and maximum contributions are obtained for

$$\overline{E}_{\text{trans}\,O,O_2} = 54.4\ \text{kJ mol}^{-1} \tag{A8}$$

and

$$\max E_{\text{trans}\,O,O_2} = 73.2\ \text{kJ mol}^{-1} , \tag{A9}$$

respectively (cf. Fig. 2 of Ref. 31). Using $T = 300$ K in Eqs. (A5) and (A6) and inserting Eqs. (A4)–(A9) into Eq. (A1), one obtains average and maximum values,

$$E_{\text{trans}} = 22.6\ \text{kJ mol}^{-1} \tag{A10}$$

and

$$\max E_{\text{trans}} = 29.3\ \text{kJ mol}^{-1} \tag{A11}$$

for the reactants. In any case, these are also the *reactive* reactants (see Ref. 39). In comparison with Eqs. (A10) and (A11), the average translational energy of thermal ($T = 300$ K) reactants in an "ideal" experiment (see Sec. V) is much smaller,

$$\text{thermal } E_{\text{trans}} = \tfrac{3}{2}\,RT = 3.8\ \text{kJ mol}^{-1} . \tag{A12}$$

The available energy of the products is evaluated by inserting Eqs. (A10), (A11), or (A12) into Eqs. (3.1) as E, $E_{\max}$ and $E(300\ \text{K})$, respectively. These three cases have been illustrated in Fig. 1.

APPENDIX B: REACTANT ORBITAL ANGULAR MOMENTUM

The average reactant orbital angular momentum is estimated classically from the relations

$$l = \tfrac{1}{2}l_{\max} = \tfrac{1}{2}\mu v b , \tag{B1}$$

where μ, v, and b are the reduced mass, the averaged velocity and the maximum impact parameter of the reactants. From Eqs. (A1) and (A10) it follows that

$$v \simeq 2300\ \text{m/s} . \tag{B2}$$

For b, we use the relations[5]

$$k = v\sigma = \pi v b^2 = 2\times 10^{-10}\ \text{cm}^3\,\text{molecule}^{-1}\,\text{s}^{-1} . \tag{B3}$$

Equations (B2) and (B3) yield the value

$$b = 0.84\ \text{Å} \tag{B4}$$

in remarkable agreement with the typical bond lengths of the system. The final result is

$$l = 2.8\times 10^{-33}\ \text{J s} \simeq 26\ \hbar . \tag{B5}$$

[1]J. Heicklen, *Atmospheric Chemistry* (Academic, New York, 1976).
[2]j denotes the rotational quantum state; J expresses the total angular momentum [cf. Eq. (3.21)].
[3]K.-H. Gericke and F. J. Comes, Chem. Phys. Lett. **74**, 63 (1980).
[4]K.-H. Gericke, F. J. Comes, and R. D. Levine, J. Chem. Phys. **74**, 6106 (1981).
[5]K.-H. Gericke and F. J. Comes, Chem. Phys. Lett. (in press). This paper gives reference to all previous measurements of the total rate coefficient of the title reaction.
[6]R. Engleman, J. Am. Chem. Soc. **87**, 4193 (1965).
[7]J. E. Butler, Faraday Discuss. Chem. Soc. **67**, 346 (1979).
[8]J. E. Butler, L. D. Talley, G. K. Smith, and M. C. Lin, J. Chem. Phys. (to be published).
[9]M. O. Rodgers, K. Asai, and D. D. Davis, Chem. Phys. Lett. **78**, 246 (1981).
[10]R. O. Levine and J. L. Kinsey, in *Atom-Molecule Collision Theory*, edited by R. B. Bernstein (Plenum, New York, 1979), p. 693, and references cited therein.
[11]H. Kaplan, R. D. Levine, and J. Manz, Chem. Phys. **12**, 447 (1976).
[12]H. Kaplan, R. D. Levine, and J. Manz, Molec. Phys. **31**, 1765 (1976).
[13]M. Kneba and J. Wolfrum, Annu. Rev. Phys. Chem. **31**, 47 (1980).
[14]D. O. Ham and J. L. Kinsey, J. Chem. Phys. **53**, 285 (1970).
[15]M. H. Mok and J. C. Polanyi, J. Chem. Phys. **53**, 4588 (1970).
[16]D. L. Thompson and D. R. McLaughlin, J. Chem. Phys. **62**, 4284 (1975).
[17]H. Elgersma and G. C. Schatz, Chem. Phys. **54**, 201 (1981).
[18]R. A. Sutherland and R. A. Anderson, J. Chem. Phys. **58**, 1226 (1973).
[19]K. R. German, J. Chem. Phys. **63**, 5252 (1975).
[20]J. Brzozowski, P. Erman, and M. Lyyra, Phys. Scr. **17**, 507 (1978).
[21]R. K. Lengel and D. R. Crosley, J. Chem. Phys. **68**, 5309 (1978).
[22]K. Schofield, J. Phys. Chem. Ref. Data **8**, 763 (1979).
[23]For simplicity of notation, primes are omitted in the following text.
[24]G. H. Dieke and H. M. Crosswhite, J. Quant. Spectrosc. Radiat. Transfer 2, 97 (1962).
[25]E. A. Moore and W. G. Richards, Phys. Scr. **3**, 223 (1971).
[26]R. J. M. Bennett, Mon. Not. R. Astron. Soc. **147**, 35 (1970).
[27]W. L. Dimpfl and J. L. Kinsey, J. Quant. Spectrosc. Radiat. Transfer **21**, 233 (1979).
[28]M. Nuss, K.-H. Gericke, and F. J. Comes, J. Quant. Spectrosc. Radiat. Transfer (in press).
[29]J. C. Tully, J. Chem. Phys. **62**, 1893 (1975).
[30]I. W. M. Smith, Discuss. Faraday Soc. **44**, 194 (1967).
[31]R. K. Sparks, L. R. Carlson, K. Shobatake, M. L. Kowalczyk, and Y. T. Lee, J. Chem. Phys. **72**, 1401 (1980).
[32]R. D. Levine and J. Manz, J. Chem. Phys. **63**, 4280 (1975).
[33]D. A. Case and D. R. Herschbach, Mol. Phys. **30**, 1537 (1975).
[34]M. Baer, J. Chem. Phys. **62**, 4545 (1975).
[35]J. N. L. Connor, W. Jakubelz, and J. Manz, Chem. Phys. **28**, 219 (1978).
[36]R. D. Levine, B. R. Johnson, and R. B. Bernstein, Chem. Phys. Lett. **19**, 1 (1973).
[37]R. B. Bernstein and R. D. Levine, Adv. At. Mol. Phys. **11**, 215 (1975).
[38]In practice we used $(\delta,\epsilon) = (X_1^2, X_2^2)$ and searched numerically for the global minimum of H in (X_1, X_2) $\{\Theta(^{16}v, {}^{16}v)\}$—space, thereby incorporating automatically two inequality constraints [Eq. (3.18)].
[39]C. Rebick, R. D. Levine, and R. B. Bernstein, J. Chem. Phys. **60**, 4977 (1974).